Polymer 49 (2008) 5199–5208

Contents lists available at ScienceDirect

Polymer

journal homepage: www.elsevier.com/locate/polymer

Z-RAFT star polymerization of styrene: Comprehensive characterization using size-exclusion chromatography

Daniel Boschmann [a], Rob Edam [b,c], Peter J. Schoenmakers [b], Philipp Vana [a,*]

[a] Institut für Physikalische Chemie, Georg-August-Universität Göttingen, Tammannstrasse 6, D-37077 Göttingen, Germany
[b] Polymer-Analysis Group, Van't Hoff Institute for Molecular Sciences, University of Amsterdam, Nieuwe Achtergracht 166, 1018 WV Amsterdam, The Netherlands
[c] Dutch Polymer Institute, P.O. Box 902, 5600 AX Eindhoven, The Netherlands

ARTICLE INFO

Article history:
Received 12 June 2008
Received in revised form
20 September 2008
Accepted 25 September 2008
Available online 4 October 2008

Keywords:
Reversible addition–fragmentation chain transfer (RAFT) polymerization
Z-RAFT star polymerization
Star polymers

ABSTRACT

Reversible addition–fragmentation chain transfer (RAFT) polymerizations of styrene in bulk at 80 °C using tri-, tetra-, and hexafunctional trithiocarbonates, in which the active RAFT groups are linked to the core via the stabilizing Z-group, were studied in detail. These Z-RAFT star polymerizations of styrene showed excellent molecular weight control up to very high monomer conversions and star sizes of more than 200 kDa. The application of high pressure up to 2600 bar was found to significantly increase the relative amount of living star polymer. Not even at very high monomer conversions and for large star molecules, a shielding effect of growing arms hampering the RAFT process could be identified. Absolute molecular weights of star polymers using a conventionally calibrated SEC setup were determined with high precision by using a mixture of linear and star-shaped RAFT agents. When using phenylethyl as the leaving R-group, well-defined star polymers that perfectly match the theoretical predictions were formed. However, when using benzyl as the leaving group, a pronounced impact of monomer conversion on the star polymer topology was observed and pure star polymers with the expected number of arms could not be obtained.

1. Introduction

The precise tailoring of macromolecules on a molecular level is a major key for controlling the polymer properties. Within this context, the control of macromolecular topology is an ongoing research theme [1]. Among these topologies, star polymers are of special interest since years, because of their distinct rheological behavior arising from their spatial shape both in solution and melt, which is exploited, e.g., in oils and lubricants for automotives [2,3], in adhesives [4], and for flocculation [5]. In addition, star polymers are becoming increasingly important for life sciences, where they e.g. find applications in the field of drug release [6], serve as unimolecular polymeric micelles [7,8], and are used as nucleic acid delivery vectors [9]. A lot of effort was put into the investigation of properties of stars [10,11] as well as into the development of new methods for their synthesis [12]. The rise of controlled radical polymerization ignited enormous research activities in the field of topological polymer design, as these methods allow the preparation of samples with narrowly distributed and controlled molecular weights of a wide array of different monomers and under various reaction conditions. Especially reversible addition–fragmentation chain transfer (RAFT) polymerization [13–17] has proven to be extremely versatile. In this method, propagating macroradicals are in equilibrium with the dormant polymeric RAFT compounds via reversible chain transfer and all chains have thus an equal probability to grow which results in relatively narrow chain length distributions. Core-first star polymers can easily be produced via RAFT polymerization when using multifunctional RAFT agents that, in addition to controlling the process, predetermine the final polymer topology [18,19]. When targeting very well-defined star polymers, a RAFT agent design has to be chosen, in which the stabilizing group (the so-called Z-group) constitutes the core (see Scheme 1) [20–25]. This Z-RAFT star polymerization approach effectively prevents extensive coupling reactions between star polymers as well as side production of linear material, which occur when connecting the RAFT group to the core via its reinitiating leaving group (the so-called R-group) [18,19,23,26–29]. For a detailed description of the mechanistic underpinnings of core-first RAFT star polymerizations, the reader is referred to Ref. [25].

In Z-RAFT star polymerization, the growing radical center sits at the end of a linear chain (i.e., the arm) and the equilibrating reaction occurs near the center of the star, where the thiocarbonylthio moieties are located throughout the entire reaction. As a matter of fact, the controlling reaction is increasingly shielded by the

* Corresponding author. Tel.: +49 551 3912753; fax: +49 551 393144.
E-mail address: pvana@uni-goettingen.de (P. Vana).

0032-3861/$ – see front matter © 2008 Elsevier Ltd. All rights reserved.
doi:10.1016/j.polymer.2008.09.048

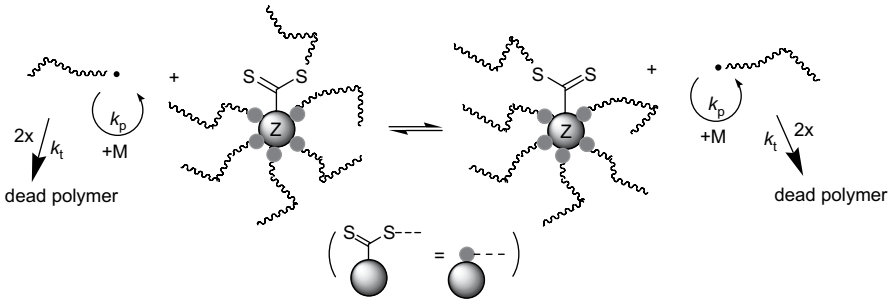

Scheme 1. Main equilibrium of Z-RAFT star polymerization.

surrounding polymer segments. It was, however, experimentally found that Z-RAFT star polymerization of acrylates is well controlled up to relatively high monomer conversions and up to star molar masses of over one million Dalton [25]. We therefore scrutinized earlier reported arguments about the detrimental steric shielding of growing arms, which was accused to increasingly hamper the RAFT process [20,21,30–32]. In order to quantify this shielding for the first time, we performed Monte Carlo simulations of polymer chain pairs that mimic the steric situation occurring in Z-RAFT star polymerization, showing that the shielding is not sufficiently large to impede the RAFT process [33,34]. We also modeled the initial transfer reaction in Z-RAFT star polymerization by pseudo-kinetic Monte Carlo simulations [35].

Our motivation for comprehensively study Z-RAFT star polymerization is driven by our efforts in designing well-defined unimolecular nano-carriers, which base on star polymers as templates [36]. We thus comprehensively studied 6-arm Z-RAFT star polymerization of various acrylates [25], in which we identified intermolecular transfer to polymer as side reaction that induces star–star coupling at high monomer conversions. Based on a detailed kinetic analysis of this transfer-to-polymer reaction, we were able to develop guidelines for poly(acrylate) stars of very uniform structure. The objective of the present work is to in-depth characterize 3-arm, 4-arm, and 6-arm Z-RAFT star polymerization of styrene in order to obtain very homogenous star polymers from this important monomer. By exploiting the distinct mechanistic features of Z-RAFT star polymerization, we develop a novel and relatively easy method for characterizing absolute molecular weights and true numbers of arms of the generated star polymers.

2. Experimental section

2.1. Chemicals

Dipentaerythritol-hexakis(3-mercaptopropionate) was obtained from Wako Chemicals and used without further purification. The initiator 1,1′-azobis(cyanocyclohexane) (ACCN, Aldrich) was used as-received. Styrene (≥99.0%, Fluka) was purified by passing through a column filled with inhibitor remover for 4-*tert*-butylcatechol (Aldrich). Column-chromatographic purification of the RAFT agent was performed using silica gel (Merck, Kieselgel 60) and technical grade *n*-pentane, ethyl acetate and CH_2Cl_2. Tetrahydrofuran was used as the eluent in size-exclusion chromatography (THF, Carl Roth, Rotipuran, stabilized with 2,6-di-*tert*-butyl-4-methylphenol). It was used as-received for all experiments using refractive index and UV detection. Unstabilized HPLC-grade THF from Biosolve (Valkenswaard, The Netherlands) was filtered over a 20 nm ceramic filter (Anodisk 47 from Whatman, Maidstone, England) and continuously purged with helium 5.0 (99.999%, Praxair, Vlaardingen, The Netherlands) for the triple-detection SEC measurements. All other chemicals were purchased from Aldrich and used without further purification.

2.2. Instrumentation

Molecular weight distributions were determined by size-exclusion chromatography (SEC) using a JASCO (Tokyo, Japan) AS-2055-plus autosampler, a Waters 515 HPLC pump (Milford, MA, USA), three PSS-SDV columns (Mainz, Germany) with nominal 5 μm particle size and pore sizes of 10^5, 10^3 and 10^2 Å, a Waters 2410 refractive index detector, a Viskotek (Houston, TX, USA) VE3210 UV/VIS detector, and THF at 35 °C as the eluent at a flow rate of 1.0 mL min^{-1}. 50 μL of polymer solution with a concentration of approximately 3 mg/mL were injected. The SEC setup was calibrated with polystyrene standards of narrow polydispersity (M_p = 410–2,000,000 g mol^{-1}) from PSS.

The triple-detector SEC setup comprised an SIL9a autosampler, LC20Advp micropump and SCL10a system controller all from Shimadzu (Kyoto, Japan). Various columns with mixed-bed particles were used (Resipore 3 μm, Minimix-C 5 μm and Minimix-B 10 μm, 250 × 4.6 mm each). All of these were obtained from Polymer Laboratories (Church Stretton, UK). The separation was performed at a flow rate of 400 μL/min and 50 μL of sample were injected. The sample solution was prepared by dissolving the polymer at a concentration of approximately 1.5 mg/mL in THF with 250 ppm butyl-hydroxylated toluene (Acros, 99%) to prevent degradation by radicals. The triple-detection array was assembled in-house (University of Amsterdam) and comprised an LC600 90° light-scattering detector (Viscotek), an on-line viscometry detector (Viscochip, Polymer Laboratories) and a differential refractive index detector (RID10a, Shimadzu). The data were acquired using a PL-datastream A/D converter (Polymer Laboratories) and processed using PL-Cirrus v3.0 software (Polymer Laboratories). Processing of the data was performed in compliance with the triple-detection principle [37,38].

Electrospray-ionization mass spectrometry (ESI-MS) experiments were carried out using a Finnigan LCQ ion trap mass spectrometer (Thermo Finnigan, San Jose, CA, USA). For further details regarding the ESI-MS setup see Ref. [39].

NMR spectroscopy was performed using a Varian Mercury 200 and a Varian Unity 300 NMR spectrometer.

Elemental analysis was carried out on a Heraeus CHN-O-Rapid Analyzer and on a METROHM 662 photometer equipped with a 636 Tiroprocessor.

2.3. RAFT agent synthesis

2.3.1. Hexyl-benzyl-trithiocarbonate, *1*

To a solution of 1-hexanethiol (1.00 g, 8.46 mmol) in 50 mL chloroform triethylamine (1.41 mL, 1.03 g, 10.2 mmol, 1.2 equiv) was added. After stirring the reaction mixture for 1 h at room

temperature, 5 mL of CS_2 and benzyl bromide (1.21 mL, 1.74 g, 10.1 mmol, 1.2 equiv) were added slowly. The mixture was stirred for 15 h and the reaction was then quenched by adding 50 mL of 10% hydrochloric acid. The organic phase was separated and washed two times with 50 mL of water and dried over Na_2SO_4. Solvent and traces of non-reacted starting materials were removed in vacuum. 2.41 g (99%) of **1** were received as a yellow liquid.

^{1}H NMR (300 MHz, $CDCl_3$) δ (ppm): 0.89 (t, $J = 7.1$ Hz, 3H, C$\underline{H}_3$–CH_2), 1.35 (m, 6H, C$\underline{H}_2$), 1.71 (p, $J = 7.2$ Hz, 2H, –S–CH_2–C$\underline{H}_2$–CH_2–), 3.37 (t, $J = 7.4$ Hz, 2H, S–C$\underline{H}_2$), 4.62 (s, 1H, C$\underline{H}_2$), 7.35 (m, 5H, $\underline{H}_{ar}$).

^{13}C NMR (300 MHz, $CDCl_3$) δ (ppm): 13.96 (C$\underline{H}_3$–CH_2), 22.45 (C$\underline{H}_2$), 27.90 (C$\underline{H}_2$), 28.56 (C$\underline{H}_2$), 31.25 (C$\underline{H}_2$), 37.03 (C$\underline{H}_2$), 41.31 (C$\underline{H}_2$), 127.69 (C$_{ar}$H), 128.65 (C$_{ar}$H), 129.22 (C$_{ar}$H), 135.07 (C$_{ar}$), 223.78 (C=S).

Mass spectrometry: m/z 285.1 ($M + H^+$), 302.2 ($M + NH_4^+$), 319.2 ($M + NH_3 + NH_4^+$), 586.3 ($2\,M + NH_4^+$).

2.3.2. Hexyl-1-phenylethyl-trithiocarbonate, **2**

The synthesis was according to that of **1**, but using (1-bromoethyl)benzene (1.39 mL, 1.88 g, 10.1 mmol, 1.2 equiv) instead of benzyl bromide. 2.49 g (97%) of **2** were received as a yellow liquid.

^{1}H NMR (300 MHz, $CDCl_3$) δ (ppm): 0.89 (t, $J = 6.7$ Hz, 3H, C$\underline{H}_3$–CH_2), 1.35 (m, 6H, C$\underline{H}_2$), 1.68 (p, $J = 7.2$ Hz, 2H, –S–CH_2–C$\underline{H}_2$–CH_2–), 1.76 (d, $J = 7.1$ Hz, 3H, C$\underline{H}_3$–CH), 3.34 (t, $J = 7.4$ Hz, 2H, S–C$\underline{H}_2$), 5.38 (q, $J = 7.1$ Hz, 1H, C$\underline{H}$), 7.35 (m, 5H, $\underline{H}_{ar}$).

^{13}C NMR (300 MHz, $CDCl_3$) δ (ppm): 13.96 (C$\underline{H}_3$–CH_2), 21.34 (C$\underline{H}_3$–CH), 22.44 (C$\underline{H}_2$), 27.90 (C$\underline{H}_2$), 28.56 (C$\underline{H}_2$), 31.25 (C$\underline{H}_2$), 36.79 (C$\underline{H}_2$), 50.03 (C$\underline{H}$), 127.63 (C$_{ar}$H), 127.67 (C$_{ar}$H), 128.60 (C$_{ar}$H), 141.16 (C$_{ar}$), 223.07 (C=S).

Mass spectrometry: m/z 299.1 ($M + H^+$), 316.2 ($M + NH_4^+$), 614.3 ($2\,M + NH_4^+$).

2.3.3. Trimethylolpropane-tris-3-(S-benzyl-trithiocarbonyl)-propanoate, **3**

To a solution of trimethylolpropane-tris-(3-mercaptopropionate) (1.00 mL, 1.21 g, 3.04 mmol) in 50 mL chloroform triethylamine (1.52 mL, 1.11 g, 10.9 mmol, 3.6 equiv) was added. After stirring the reaction mixture for 1 h at room temperature 5 mL of CS_2 and benzyl bromide (1.30 mL, 1.87 g, 10.9 mmol, 3.6 equiv) were added slowly. The mixture was stirred for 15 h and the reaction was then quenched by adding 50 mL of 10% hydrochloric acid. The organic phase was separated and washed two times with 50 mL of water and dried over Na_2SO_4. Solvent and traces of non-reacted starting materials were removed in vacuum. 2.73 g (99%) of **3** were received as a yellow liquid.

^{1}H NMR (300 MHz, $CDCl_3$) δ (ppm): 0.88 (t, $J = 7.6$ Hz, 3H, C$\underline{H}_3$), 1.47 (q, $J = 7.6$ Hz, 2H, C$\underline{H}_2$), 2.79 (t, $J = 7.0$ Hz, 6H, C$\underline{H}_2$), 3.62 (t, $J = 7.0$ Hz, 6H, C$\underline{H}_2$), 4.05 (s, 6H, C$\underline{H}_2$), 4.61 (s, 6H, C$\underline{H}$), 7.32 (m, 15H, $\underline{H}_{ar}$).

^{13}C NMR (300 MHz, $CDCl_3$) δ (ppm): 7.34 (C$\underline{H}_3$), 23.02 (C$\underline{H}_3$–CH), 31.23 (C$\underline{(CH_2)_3}$), 33.07 (C$\underline{H}_2$), 33.13 (C$\underline{H}_2$), 40.73 (CH_2), 64.12 (C$\underline{H}_2$), 127.79 (C$_{ar}$H), 128.69 (C$_{ar}$H), 129.24 (C$_{ar}$H), 134.79 (C$_{ar}$), 170.96 (C=O), 221.98 (C=S).

Mass spectrometry: m/z 897.07 ($M + H^+$), 914.10 ($M + NH_4^+$).

An alternative pathway for the synthesis of **3** is given by Stenzel and co-workers [40].

2.3.4. Trimethylolpropane-tris-(3-(S-phenylethyl-trithiocarbonyl)propanoate), **4**

The synthesis was according to that of **3**, but using (1-bromoethyl)benzene (1.50 mL, 2.02 g, 10.9 mmol, 3.6 equiv) instead of benzyl bromide. 2.86 g (99%) of **4** were received as a yellow liquid.

^{1}H NMR (300 MHz, $CDCl_3$) δ (ppm): 0.87 (t, $J = 7.6$ Hz, 3H, C$\underline{H}_3$), 1.45 (q, $J = 7.6$ Hz, 2H, C$\underline{H}_2$) 1.75 (d, $J = 7.1$ Hz, 9H, C$\underline{H}_3$–CH), 2.76 (t, $J = 7.0$ Hz, 6H, C$\underline{H}_2$), 3.57 (t, $J = 7.0$ Hz, 6H, C$\underline{H}_2$), 4.02 (s, 6H, C$\underline{H}_2$), 5.32 (q, $J = 7.1$ Hz, 3H, C$\underline{H}$), 7.32 (m, 15H, $\underline{H}_{ar}$).

^{13}C NMR (300 MHz, $CDCl_3$) δ (ppm): 7.33 (C$\underline{H}_3$), 21.32 (C$\underline{H}_3$–CH), 26.79 (C$\underline{H}$), 30.95 (C$\underline{(CH_2)_3}$), 33.08 (C$\underline{H}_2$), 33.15 (C$\underline{H}_2$), 40.72 (CH_2), 50.36 (C$\underline{H}_3$), 64.07 (C$\underline{H}_2$), 127.66 (C$_{ar}$H), 127.73 (C$_{ar}$H), 128.64 (C$_{ar}$H), 140.92 (C$_{ar}$), 221.98 (C=S).

Mass spectrometry: m/z 956.14 ($M + NH_4^+$).

2.3.5. Pentaerythritol-tetrakis-(3-(S-benzyl-trithiocarbonyl)-propanoate), **5**

Compound **5** was synthesized according to Mayadunne et al. [19].

2.3.6. Pentaerythritol-tetrakis-(3-(S-1-phenylethyl-trithiocarbonyl)propanoate), **6**

To a solution of pentaerythritol-tetrakis(3-mercaptopropionate) (0.71 mL, 1.44 g, 5.00 mmol) in 100 mL chloroform triethylamine (5.53 mL, 4.04 g, 40.0 mmol, 8 equiv) was added. After stirring the reaction mixture for 1 h at room temperature 10 mL of CS_2 and (1-bromoethyl)benzene (3.02 mL, 4.07 g, 22.0 mmol, 4.1 equiv) were added slowly. The mixture was stirred for 15 h and afterwards the reaction was quenched by adding 100 mL of 10% hydrochloric acid. The organic phase was separated and washed two times with 100 mL of water and dried over Na_2SO_4. Solvent was removed in vacuum and the crude product was purified on silica with CH_2Cl_2 ($R_f = 0.38$) as eluent. 2.98 g (49%) of **6** were received as yellow oil.

^{1}H NMR (200 MHz, $CDCl_3$) δ (ppm): 1.75 (d, $J = 7.1$ Hz, 12H, C$\underline{H}_3$–CH), 2.76 (t, $J = 7.0$ Hz, 8H, C$\underline{H}_2$), 3.56 (t, $J = 7.0$ Hz, 8H, C$\underline{H}_2$), 4.02 (s, 8H, C$\underline{H}_2$), 5.32 (q, $J = 7.1$ Hz, 4H, C$\underline{H}$), 7.32 (m, 20H, $\underline{H}_{ar}$).

^{13}C NMR (300 MHz, $CDCl_3$) δ (ppm): 21.32 (C$\underline{H}_3$–CH), 30.92 (C$\underline{(CH_2)_3}$), 32.98 (C$\underline{H}_2$), 40.92 (CH_2), 50.36 (C$\underline{H}_3$), 62.52 (C$\underline{H}_2$), 127.67 (C$_{ar}$H), 127.73 (C$_{ar}$H), 128.63 (C$_{ar}$H), 140.87 (C$_{ar}$), 170.76 (C=O), 221.89 (C=S).

Mass spectrometry: m/z 1226.13 ($M + NH_4^+$).

2.3.7. Dipentaerythritol-hexakis-(3-(S-benzyl-trithiocarbonyl)-propanoate), **7**

Compound **7** was synthesized as recently reported by Johnston-Hall and Monteiro [41].

2.3.8. Dipentaerythritol-hexakis-(3-(S-1-phenylethyl-trithiocarbonyl)propanoate), **8**

To a solution of dipentaerythritol-hexakis(3-mercaptopropionate) (3.915 g, 5.00 mmol) in 200 mL chloroform triethylamine (6.32 mL, 6.07 g, 60.0 mmol, 12 equiv) was added. After stirring the reaction mixture for 1 h at room temperature 50 mL of CS_2 and (1-bromoethyl)benzene (4.78 mL, 6.48 g, 60.0 mmol, 12 equiv) were added slowly. The mixture was stirred for 15 h and afterwards the reaction was quenched by adding 100 mL of 10% hydrochloric acid. The organic phase was separated and washed two times with 100 mL of water and dried over Na_2SO_4. The solvent was evaporated in vacuum. The crude product was purified via column chromatography on silica gel using pentane:ethyl acetate (3:1; $R_f = 0.38$) as eluent. 4.48 g (48%) of **8** were received as yellow oil.

^{1}H NMR (300 MHz, $CDCl_3$) δ (ppm): 1.75 (d, $J = 7.1$ Hz, 12 H, C$\underline{H}_3$), 2.76 (t, $J = 7.0$ Hz, 12H, C$\underline{H}_2$), 3.56 (t, $J = 7.0$ Hz, 12H, C$\underline{H}_2$), 4.11 (s, 12H, C$\underline{H}_2$), 5.32 (q, $J = 7.1$ Hz, 6H, C$\underline{H}$), 7.25 (m, 30H, $\underline{H}_{ar}$).

^{13}C NMR (200 MHz, $CDCl_3$) δ (ppm): 21.33 (C$\underline{H}_3$), 30.79 (C$\underline{(CH_2)}$), 30.93 (C$\underline{H}_2$), 32.99 (C$\underline{H}_2$), 42.92 (CH_2), 50.37 (C$\underline{H}_2$), 62.53 (C$\underline{H}_2$), 127.68 (C$_{ar}$H), 127.74 (C$_{ar}$H), 128.64 (C$_{ar}$H), 140.88 (C$_{ar}$), 170.77 (C=O), 221.98 (C=S).

Elemental analysis: C, 52.81; H, 5.08; S, 30.95 (theor.). C, 53.32; H, 5.38; S, 29.95 (exp.).

2.4. Polymerizations

Styrene was degassed via three freeze–pump–thaw cycles, transferred along with RAFT agent and initiator into an argon-filled

glove box (oxygen content below 1.5 ppm), where stock solutions of 10 mL monomer, initiator (ACCN), and RAFT agent or RAFT agent mixtures were prepared. For the ambient pressure experiments, ten samples of each stock solution were filled into individual glass vials and sealed with Teflon/rubber septa. The vials were subsequently inserted into a block heater, thermostated at 80 ± 0.1 °C. The samples were removed after preset time intervals and the reactions were stopped by cooling the solutions in an ice bath. The reaction times were up to 144 h. Polymerizations up to pressures of 2600 bar were performed in in-house-made pressure cells. For details see ref. [42]. Monomer to polymer conversions were determined gravimetrically.

3. Results and discussion

For our studies of Z-RAFT star polymerization of styrene, we chose multifunctional trithiocarbonates as RAFT agents (see Chart 1). Trithiocarbonates become increasingly popular as RAFT agents, due to their facile preparation and due to the absence of potentially disturbing rate retardation effects, which are observed with more reactive RAFT agents such as dithiobenzoates [43]. Mayadunne et al. [19] were the first who introduced pentaerythritol-based multifunctional trithiocarbonates as Z-RAFT star agents. Since then, the synthesis protocols for this class of star-shaped RAFT agents were adapted by us [25] and others [41], providing access to bi-, tri-, tetra- and hexafunctional mediating agents. Other trithiocarbonate-type Z-RAFT star agents used in styrene polymerization were based on β-cyclodextrin cores [20], on hyperbranched polymer cores [30], and on dendrimers [24]. Multifunctional dithiobenzoates for usage in styrene polymerization were constructed as dendrimers [21] and as 1,3,5-benzene-tri-dithiocarboxylic-esters [32]. All these RAFT agents used for Z-RAFT star polymerization of styrene were decorated with a benzyl-moiety as the reinitiating leaving group. This is surprising, as it is well understood that benzyl as leaving group results in a relatively low apparent chain transfer coefficient of the associated RAFT agent in styrene polymerization, both with trithiocarbonates [44] and with dithiobenzoate [45]. This is due to the relatively high energy of the benzyl radical, which slows down the fragmentation rate of the initial intermediate radical and speeds up the undesired back-transfer within the pre-equilibrium in comparison to monomer addition. This scenario results in a pronounced so-called hybrid behavior [46], which describes the formation of relatively high molecular weights of the resulting polymer after only negligible monomer conversion, *X*, that is, experimental molecular weight vs. *X* plots show a significant intercept instead of crossing the origin. The resulting polydispersities are consequently significantly higher than in systems with more effective pre-equilibriums [45]. The preference for benzyl as leaving group seen in every study into Z-RAFT star polymerization of styrene performed so far is obviously due to the easiness of the associated RAFT agent synthesis. In an effort to optimize this polymerization system, we consequently implemented phenylethyl as leaving group, which induces a more effective pre-equilibrium in styrene polymerization [44]. It should be noted that benzyl as the leaving group may unfold sufficient transfer activity in other monomer systems, such as acrylates, due to a pronouncedly different fragmentation selectivity of the RAFT intermediate of the pre-equilibrium.

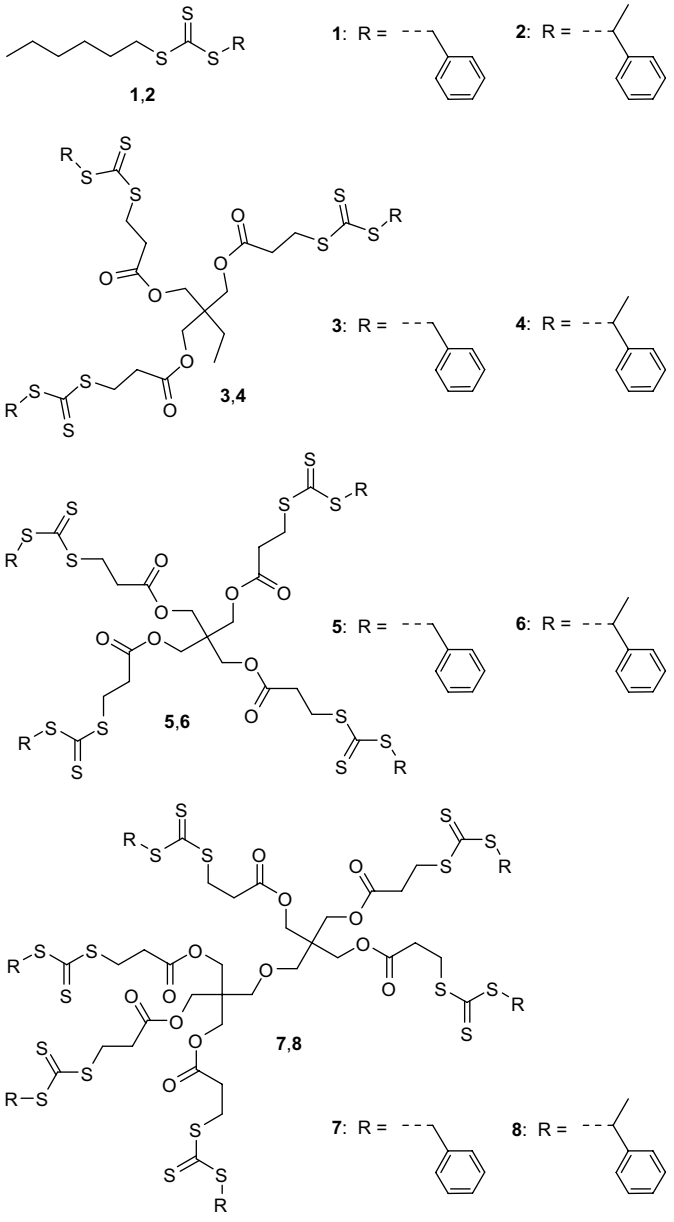

Chart 1. Mono-, tri-, tetra-, and hexafunctional RAFT agents used in this study.

When using RAFT agents **1**, **3**, **5**, and **7** at, e.g., ca. 1 mmol L^{-1} of RAFT-group concentration, intercepts of the experimental number average molecular weight, $\overline{M}_n$, vs. *X* traces of around 8000 g mol^{-1} were observed (not shown). This finding is in agreement with literature reports about benzyltrithiocarbonate-mediated styrene polymerizations, in which similar intercepts were found [20,32,47]. The Z-RAFT star polymerization of styrene using RAFT agents **4**, **6**, and **8**, which carry a phenylethyl moiety revealed – as anticipated – that the hybrid behavior is largely reduced in comparison to benzyl as the leaving group. Nevertheless, a minor hybrid behavior could still be observed, especially with low RAFT agent concentrations. In Fig. 1a, the intercept values $\overline{M}_{n,0\%}$ are depicted on the example of **8**-mediated 6-arm star polymerization. The other RAFT agents showed very similar behavior. It can clearly be seen that the intercept is below 4000 g mol^{-1}, even for RAFT agent concentrations below 1 mmol L^{-1}, and approaches zero with increasing RAFT agent concentration. The polymerizations were performed at 80 °C, which we identified as optimal. Since styrene is a slowly propagating monomer [48] and usage of vast amounts of initiator is not advisable, as it drastically increases the amount of terminated polymer, reaction times in which full monomer conversion were reached lasted up to several days. It was hence necessary to use the slowly decomposing initiator ACCN, which has about the same fragmentation rate at 80 °C as has AIBN at 60 °C [49].

It is tempting to use the intercepts for obtaining average chain-transfer constants for the initial RAFT step via plotting the inverse number average degree of polymerization at zero monomer

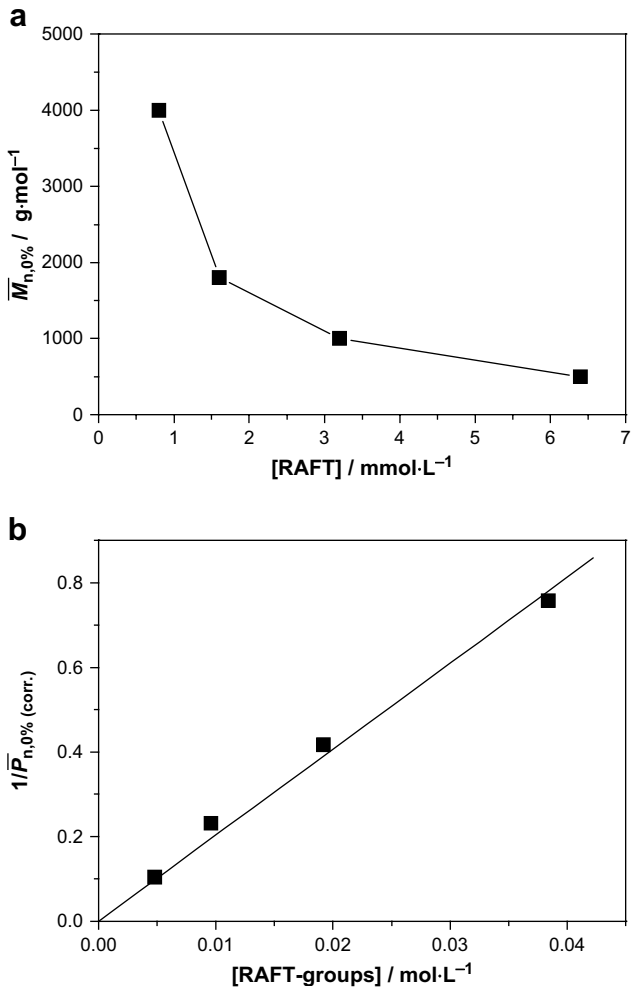

Fig. 1. (a) Intercepts of apparent number average molecular weight from conventional calibration using linear standards, $\overline{M}_n$ vs. X traces in **8**-mediated styrene bulk polymerization (6-arm star polymerization) vs. RAFT agent concentrations at 80 °C using ACCN ($c_{ACCN} = 3$ mmol L^{-1}) as the initiator. (b) Inverse degree of polymerization (corrected by K taken from Fig. 9 according to the procedure described in the text) at zero monomer conversion (extrapolated values) of star arm polymer vs. the concentration of trithiocarbonate groups. The line indicates the best linear fit, forced through the origin.

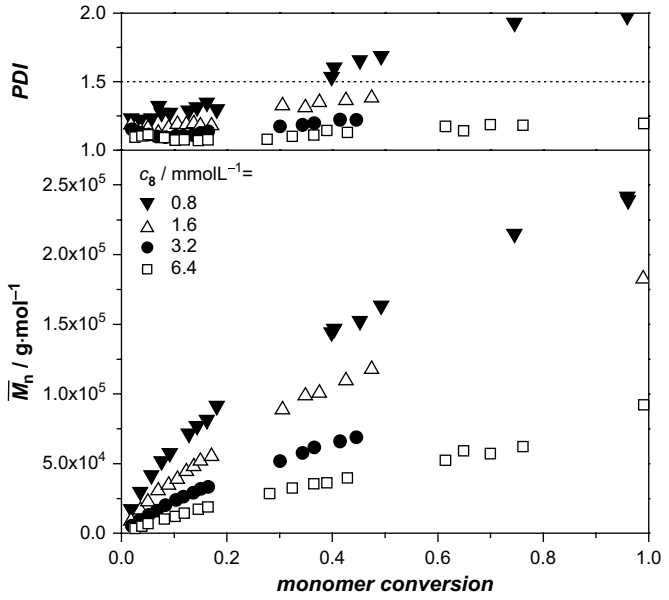

Fig. 2. Polydispersity index, PDI, and apparent number average molecular weight from conventional calibration using linear standards, $\overline{M}_n$, vs. monomer conversion in **8**-mediated styrene bulk polymerization (6-arm star polymerization) at various RAFT agent concentrations at 80 °C using ACCN ($c_{ACCN} = 3$ mmol L^{-1}) as the initiator.

conversion, $1/\overline{P}_{n,0\%}$, against the RAFT agent concentration, as has been demonstrated by Barner-Kowollik and co-workers [50,51]. However, this approach is beset by problems in the case of star polymers, as the molecular weights obtained using SEC calibrated with linear standards differ significantly from true molecular weights. This needs to be addressed in the evaluation procedure, which will be presented below.

The performed Z-RAFT star polymerizations using 3-, 4-, and 6-armed RAFT agents exhibited very well-controlled behavior up to full monomer conversion, as is exemplified on **8**-mediated 6-arm star polymerization of styrene (see Fig. 2). Polydispersities show minimal values of 1.07 at $X = 20\%$ when using RAFT agent concentrations of 6.4 mmol L^{-1}, which refer to 3.8×10^{-2} mol L^{-1} of trithiocarbonate moieties. The slight curvature of the $\overline{M}_n$ vs. X traces originates from continued formation of dead chains (see below).

Full molecular weight distributions of the formed star polymers, as exemplified on **6**-mediated styrene polymerization (4-arm star polymerization) (see Fig. 3) are narrow and unimodal, as expected for a well-controlled polymerization. This is in contrast to Z-RAFT star polymerization of acrylates, in which star–star coupling side reactions were observed after intermediate values of X [25]. The polymerization behaviors of **4**-, **6**-, and **8**-mediated polymerizations of styrene were very similar to each other, thus, only demonstrating examples are presented.

RAFT polymerization requires continuous delivery of initiating radicals, whereby dead polymer is formed throughout the entire polymerization. Especially at low RAFT agent concentrations and with slowly propagating monomers, such as styrene, the amount of terminated polymer can become significant. In Z-RAFT star polymerization, termination occurs between two growing arms (see Scheme 1), generating dead polymer that at maximum, in the case of termination via combination, has double the chain length of one arm polymer, which is lower than the degree of polymerization of the complete star. Dead polymer consequently occurs completely at the low molecular weight side of the living star polymer, as demonstrated in Fig. 4, in which 4-arm star polymer is presented

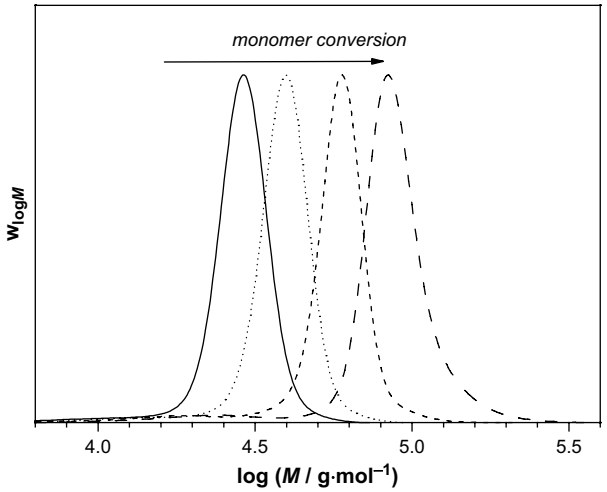

Fig. 3. SEC distributions, w_{logM}, of polystyrene samples produced in **6**-mediated ($c_6 = 9.6$ mmol L^{-1}) styrene bulk polymerization (4-arm star polymerization) at 80 °C using ACCN ($c_{ACCN} = 3$ mmol L^{-1}) as the initiator, after monomer conversion of 30% (PDI = 1.06), 46% (PDI = 1.08), 73% (PDI = 1.11) and after full monomer conversion (PDI = 1.17).

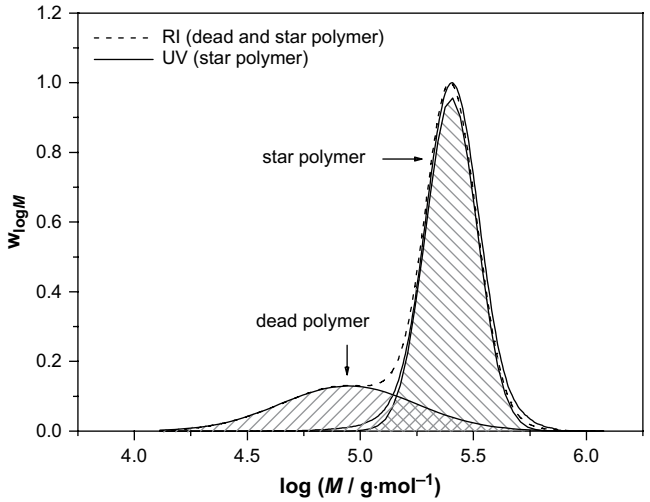

Fig. 4. SEC distribution, w_{logM}, of polystyrene samples produced in **6**-mediated ($c_{\mathbf{6}} = 0.8$ mmol L^{-1}) styrene bulk polymerization (4-arm star polymerization) at 80 °C using ACCN ($c_{ACCN} = 3$ mmol L^{-1}) as the initiator, after 26% of monomer conversion. (—) RI detection (overall molecular-weight distribution); (—) via UV detection at 330 nm (trithiocarbonate end groups, indicating living star polymer). The UV signal was corrected according to Ref. [25] to allow comparison. The RI signal was subjected to multi-Gaussian fitting (striped patterns).

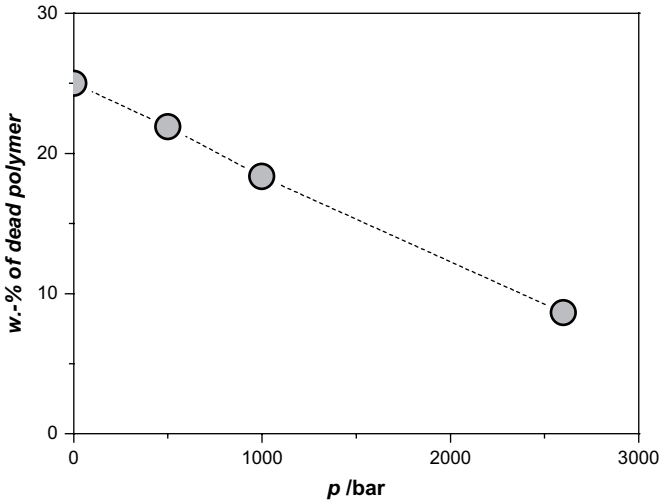

Fig. 5. Weight percent of dead polymer, *w.-%*, vs. applied pressure in **6**-mediated ($c_{\mathbf{6}} = 1.2$ mmol L^{-1}) styrene bulk polymerization (4-arm star polymerization) at 80 °C using ACCN ($c_{ACCN} = 3$ mmol L^{-1}) as the initiator after 25% of monomer conversion.

that has been formed in the presence of relatively low RAFT agent concentration. UV detection set to 330 nm has been used to selectively detect the trithiocarbonyl group, i.e., the living star polymer, which – after appropriate correction [25] – can be related to the molecular weight distribution from RI detection, which includes both the living and the dead polymer.

It is clear that the formation of dead polymer is an obstacle for obtaining pure and narrowly dispersed star polymer. Terminated linear polymer can either be separated from the star polymer, e.g., via selective extraction [21], or its formation can be minimized during the process via the following strategies: (i) the polymerizations can be performed at high RAFT agent concentrations, which suppress the relative influence of terminated polymer. The maximum molecular weight, however, which can be achieved thereby, is restricted. (ii) When performing the RAFT polymerization at very low radical concentrations, the kinetic chain length becomes long, i.e., termination is suppressed in comparison to propagation. This lowering of dead polymer, however, is on the expense of polymerization rate, which can thus become considerable. The low initiator concentrations used in the present study, for instance, yielded well-defined star polymers with relatively low amounts of dead polymer; the reaction times, however, were several days (e.g., see gaps in Fig. 2 which indicate overnight periods). (iii) The kinetic chain length can also be stretched by applying high pressure, as we demonstrated earlier for cumyldithiobenzoate-mediated polymerizations [42]. The impact of high pressure becomes evident when quantifying the amount of dead polymer. Due to the clear separation of dead and living polymer in Z-RAFT star polymerization (see Fig. 4), these species can roughly be separated via multi-Gaussian fitting, yielding estimates for the weight fraction of terminated polymer.

Inspection of Fig. 5 clearly shows that the fraction of dead polymer is largely reduced when applying high pressure. Since samples are compared that were taken after identical monomer conversions, they have almost identical molecular weights. As high pressure increases the value of k_p/k_t, the rate of polymerization is increased as well, that is, the reaction times for obtaining identical monomer conversion is significantly reduced with increasing pressure. It goes without saying that the decreased amount of terminated polymer is also reducing the polydispersity of the overall generated polymer; the impact on the polydispersity of the living star polymer, which may be anticipated due to the pressure dependence of the individual RAFT reactions, however, remains too small to be detected unambiguously. For a detailed discussion of the pressure effect in RAFT polymerization, the reader is referred to Ref. [42].

In order to further characterize the Z-RAFT star polymerizations of styrene, we compared molecular weights from SEC measurements to theoretical values, $\overline{M}_n^{theo}$, which were calculated using the following equation.

$$\overline{M}_n^{theo} = \frac{X \cdot c_M^0 \cdot M_{monomer}}{c_{RAFT}^0 + c_I^0 \cdot d \cdot f \cdot \left(1 - e^{-k_d \cdot t}\right)} + M_{RAFT} \qquad (1)$$

with the monomer to polymer conversion, X, the initial monomer concentration, c_M^0, the initial RAFT agent concentration, c_{RAFT}^0, the initial initiator concentration, c_I^0, the molecular weights of monomer, $M_{monomer}$, and of RAFT agent, M_{RAFT}, with d being the number of chains that are generated in the termination process ($d \approx 1$ for styrene), with the initiator decomposition rate coefficient, k_d ($k_d = 1.02 \times 10^{-5}$ s^{-1} for ACCN at 80 °C [49]), and the initiator efficiency f, which we recently determined to be around unity [52]. In many reported studies, a simplified version of Eq. (1) is used, which does not account for the continuous production of chains via initiation and yields straight lines for $\overline{M}_n^{theo}$ vs. X traces. Such approach is, however, not advisable for slowly propagating monomers, such as styrene, where significant amounts of additional chains are produced before elevated monomer conversions are reached.

Inspection of Fig. 6 reveals that almost perfect agreement between molecular weights from SEC and predicted values is found up to very high X values when using the monofunctional trithiocarbonate **2** to obtain linear polymer. When using star-shaped RAFT agents, however, a systematic deviation from theoretical values is observed; the magnitude of the deviation increases with increasing numbers of arms. This effect is well understood [53] and relates to the fact that star polymers exhibit a smaller hydrodynamic volume in a good solvent than the linear polymers of identical molecular weight that served as molecular-weight calibrants for the SEC setup. Star polymers are consequently eluted later (corresponding to smaller hydrodynamic volumes). If molecular weights were to be calculated using conventional (linear) standards, the obtained values would be too low. Since the studied Z-RAFT star polymerizations of styrene exhibit well-controlled behavior, *i.e.* steadily

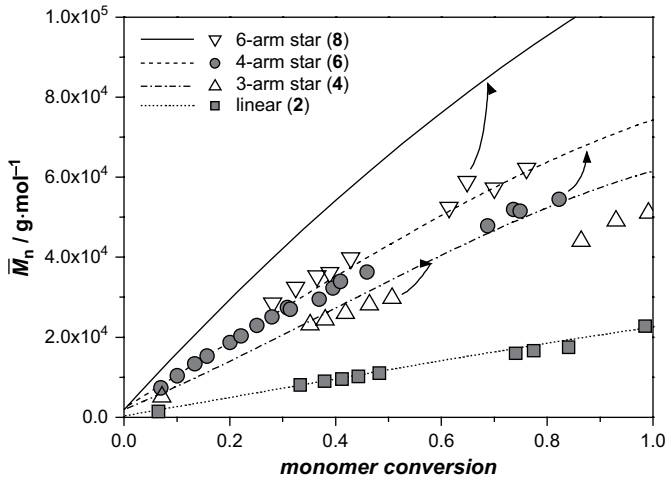

Fig. 6. Number average molecular weight, $\overline{M}_n$, by conventionally calibrated SEC vs. monomer conversion in styrene bulk polymerizations at 80 °C using ACCN ($c_{ACCN} = 3$ mmol L^{-1}) as the initiator and **2**, **4**, **6**, and **8** (see Chart 1) as the RAFT agents. The concentration of trithiocarbonate groups was 38 mmol L^{-1} in all cases. Lines indicate the theoretical molecular weights, calculated via Eq. (1).

increasing molecular weights and low polydispersities up to very high monomer conversion (see Figs. 2 and 6), we conclude that the controlling reaction of macroradicals and RAFT groups near the center of the core is fast enough to guarantee an efficient RAFT equilibrium, independent of the number (if ≤6) and length of the growing arms. This finding is in line with our recent simulation studies [33,34]. Apparent ceasing of star polymer growth, reported by Stenzel and co-workers [20,24,30,31] and Gnanou and co-workers [32], which was attributed to a loss of RAFT control due to shielding effects, was possibly more likely due to large fractions of dead polymer because of high initiator concentrations and high reaction temperatures, and due to arm cleavage via RAFT reaction of small initiating radicals at elevated monomer conversions, which counterbalance the star polymer growth.

The good agreement between experimental $\overline{M}_n$ and theoretical $\overline{M}_n^{theo}$ vs. X plots for monofunctional RAFT agent (see Fig. 6) indicates that Eq. (1) is valid and that the curvature of the plot is due to the formation of dead chains. The deviations for the star polymers have thus to be attributed to a different effect, i.e., the reduced hydrodynamic volume of star polymers. In order to prove this assumption, the absolute molecular weights of the star polymers need to be known. This can either be done via light-scattering detection (see below), which is challenging for polymer of low and medium molecular weights and moreover may not be available in every laboratory, or via arm cleavage yielding linear polymer that can be measured via conventionally calibrated SEC [19,23,25]. We found that arm cleavage experiments, either via treatment with amines or radical sources, give not well reproducible results and are prone to several side reactions that alter the molecular weight distribution. For an approximate characterization of star polymers, this might be sufficient; for a more detailed study, however, methods with higher precision are required. We hence developed a very straightforward method, which enables to measure absolute molecular weights of star polymers from Z-RAFT star polymerization via conventionally calibrated SEC.

When performing a RAFT polymerization using a mixture of monofunctional and star-shaped Z-RAFT agent, two RAFT equilibriums are established, which are interlinked via the growing macroradicals, *i.e.* the individual arms (see Scheme 2). Because of the controlled nature of RAFT polymerization, all macroradicals in the system have approximately the same chain length and, during the polymerization, either add to a linear polymeric RAFT agent

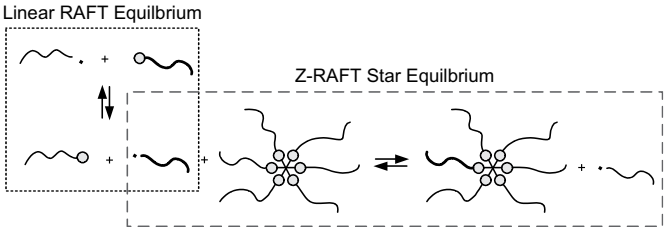

Scheme 2. The interdigitated equilibriums of simultaneously proceeding linear and Z-RAFT star polymerization. Thiocarbonylthio moieties are indicated by circles.

(linear RAFT equilibrium) or to a living star polymer (Z-RAFT star equilibrium). This situation implies that linear polymer and arm polymer within the star at any time have identical average molecular weights, as they are constantly exchanged via the RAFT equilibriums.

It should be noted that this approach works best when all RAFT groups in the system show similar chain transfer reactivity, independent whether they are part of the mono- or the multifunctional RAFT agent, which guarantees an even distribution of arms between the free and the linked state. This can generally be achieved by using identical RAFT agent moieties both in the mono- and the multifunctional agents. Molecular-weight distributions of polymer formed in the presence of a mixture of mono- and a multifunctional RAFT agent are distinctively bimodal, as shown in Fig. 7 on the example of a 4-arm star polymerization. For such trithiocarbonate-mediated systems, the transfer activity was – as required for this method – found as being independent on the RAFT agent functionality [35]. Both the linear polymer (arms) and the star polymer increase steadily in molecular weight with monomer conversion. Since the trithiocarbonate-group concentration was chosen to be identical for both RAFT agents, the weight fraction of both types of polymer is identical, too. It can also be seen that the polydispersity of the star polymer is smaller than that of the

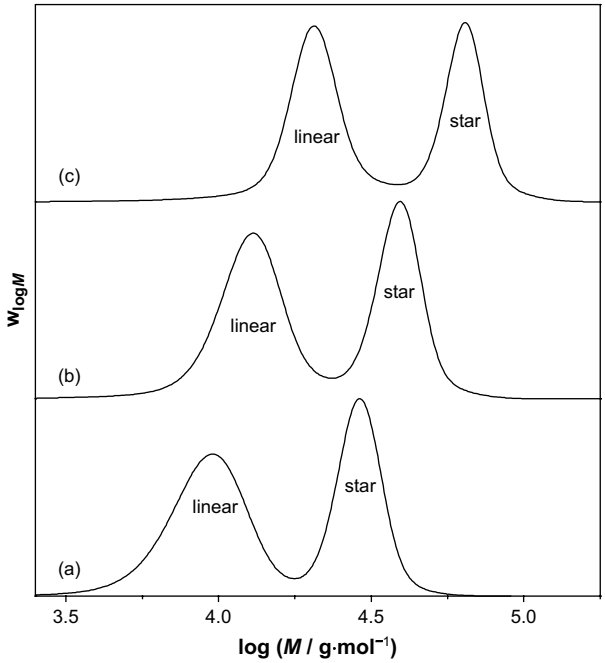

Fig. 7. Molecular weight (SEC) distributions, $w_{\log M}$, of polystyrene (M are apparent molecular weights from conventional calibration using linear standards) generated in the presence of 19 mmol L^{-1} of linear RAFT agent **2**, 4.8 mmol L^{-1} of tetrafunctional RAFT agent **6**, and 3.0 mmol L^{-1} ACCN as the initiator at (a) 29%, (b) 43%, and (c) 81% of monomer conversion.

individual arms, which is due to the arbitrary combination of dispersed arm polymer within one star polymer molecule.

As the molecular weight of the linear arm polymer can accurately be determined via conventionally calibrated SEC, the true number average molecular weight of the star polymer can be calculated by multiplying the number average molecular weight of one arm by the number of arms of the respective star. Both the arm and star polymers are narrowly distributed due to the RAFT process. Thus, the number average molecular weights are well represented by the peak molecular weight. This implies that by dividing the peak molecular weight of the star polymer, $M_{p,star}$, by the peak molecular weight of the linear arm polymer, $M_{p,arm}$, the apparent number of arms, as shown in Fig. 8 for 3-arm, 4-arm, and 6-arm stars, can be calculated.

It can clearly be seen that the apparent number of arms is always smaller than the expected number, which reflects the contracted nature of the star polymers in comparison to linear chains. 6-Arm stars appear to have only 3.94 arms, 4-arm stars appear to have only 3.05 arms, and 3-arm stars seem to have only 2.58 arms. Further important information drawn from Fig. 8 is that the apparent numbers of arms remain constant throughout the polymerization. This means that the topology of the star polymer remains unaltered, independent of monomer conversion, i.e., star–star coupling or arm cleavage reactions at elevated X values are absent. From the apparent number of arms, a correction factor K for the SEC setup was calculated by dividing the theoretical number of arms (f_{theory}) by the apparent number of arms (f_{app}) (see Eq. (2)). This factor relates absolute molecular weight of a star polymer M_{star} to that of a linear polymer M_l eluting at the same hydrodynamic volume and is depicted in Fig. 9 as function of number of arms, f. (Comparison of polymers at identical molecular weight or identical hydrodynamic volume is in the following indicated by a subscript M or V respectively.)

$$K = \left(\frac{f_{theory}}{f_{app}}\right) = \left(\frac{M_{star}}{M_l}\right)_V \tag{2}$$

Branching ratios describing the reduction of the radius of gyration, R_g, or of the hydrodynamic radius, R_H, of branched polymers have been subject of research for quite some time. In order to compare our results, which were obtained via SEC separation

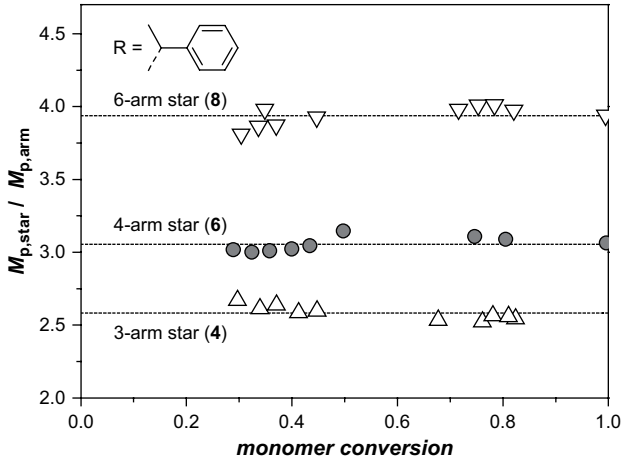

Fig. 8. Ratio of peak molecular weights of star polymer and peak molecular weights of linear arm polymer ($M_{p,star}/M_{p,arm}$), as obtained by conventionally calibrated SEC vs. monomer conversion for styrene bulk polymerizations at 80 °C using ACCN ($c_{ACCN} = 3$ mmol L^{-1}) as the initiator and mixtures of **2** and **4** (3-arm star polymerization), **2** and **6** (4-arm star polymerization), and **2** and **8** (6-arm star polymerization). The overall trithiocarbonate-group concentration was around 38 mmol L^{-1} for all samples with approximately half the number of RAFT groups belonging to multifunctional RAFT agents. Horizontal lines indicate the average value.

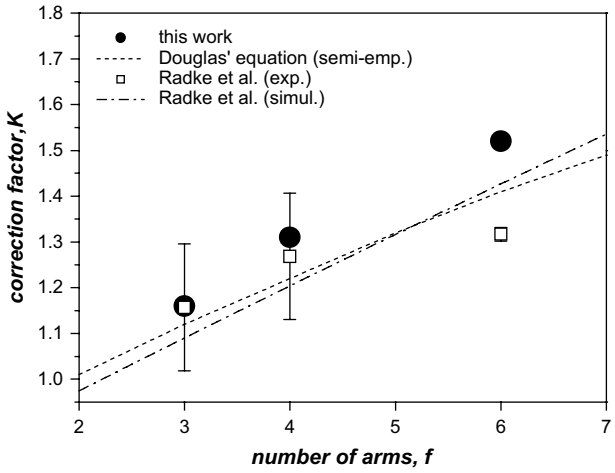

Fig. 9. Correction factor, K, for calculating absolute molecular weights of star polymers from values obtained using SEC with conventional calibration with linear standards. Closed circles: data from this work; dashed line: semi-empirical equation by Douglas et al. [54]; open squares: mean values of experimental data collated by Radke et al. [55], error bars are standard deviations; dashed-dotted line: computer simulations by Radke et al. [55,56].

without on-line light scattering or viscosity detection, with branching ratios from literature that are usually reported for identical molar mass, a calculation procedure, e.g., starting from the viscosity branching ratio, is required. The viscosity branching ratio g' (see Eq. (3))

$$g' = \left(\frac{[\eta_{br}]}{[\eta_l]}\right)_M \tag{3}$$

is relating intrinsic viscosity $[\eta]$ at identical mass of branched (index br) and linear (index l) polymer and can be rewritten using the theory of universal calibration [57], yielding Eq. (4), which relates molecular weight of the linear and branched polymers of identical hydrodynamic volume.

$$g' = \left(\frac{M_l}{M_{br}}\right)_V^{a+1} \tag{4}$$

The exponent a in Eq. (4) is the Mark–Houwink coefficient of the linear polymer, i.e., 0.700 for polystyrene in THF at 30 °C [58] as used in the present study. The correction factor K can then be compared to branching ratio data from other studies by combining Eqs. (2) and (4), resulting in Eq. (5).

$$K = g'^{(-1/(a+1))} \tag{5}$$

A prominent data set was reported by Douglas and co-workers [54], who calculated g' for regular stars using the theoretical model by Stockmayer and Fixman [59]. They found a semi-empirical relation (6) which describes the viscosity branching ratio for regular stars in a good solvent best with $\varepsilon = 0.58$, which is an empirical form factor.

$$g' = \left(\frac{3f-2}{f^2}\right)^{\varepsilon}\left(\frac{1-0.276-0.015(f-1)}{1-0.276}\right) \tag{6}$$

Based on this, Tsitsilianis et al. [60] described that the functionality of regular stars can be calculated using SEC and Eqs. (4) and (6), that is, they used an approach that is similar to the one described in this work. Inspection of Fig. 9 shows that the values obtained in the present study are in relatively good agreement with semi-empirical g' values reported by Douglas et al. [54], calculated by Eq. (6) and transformed to K values via Eq. (5). Interestingly, the trend of our

data is well matching that of Douglas' data, although the absolute values of our results are slightly higher.

Correction factors *K* for usage in conventionally calibrated SEC were also reported by Radke et al. [55,56], who collated experimental contraction factors of star polymers that were generated by various techniques and performed simulations of star polymer shapes. These data are also plotted in Fig. 9. It can be seen that our results fit excellently to the averaged experimental values by Radke et al. [55] for 3-arm stars (7 reported data points) and 4-arm stars (6 reported data points) and that the simulated data by Radke et al. [55,56] nicely matches Douglas' equation (6). A somewhat higher discrepancy can be seen for 6-arm stars: Our data are slightly higher than the simulated data by Radke et al. as well as the semi-empirical data by Douglas et al., whereas the experimental values reported by Radke et al. are significantly lower than these calculated values. This data point originates from two samples only, which were generated via coupling of pre-polymer and subsequent separation of grafted polymers having various arm numbers. These laborious procedures might be a source of uncertainty. Since our method prepares star and arm polymer simultaneously in a simple and straightforward fashion, the herein reported data are possibly more precise. It is also gratifying to note that our data almost perfectly follow the relative trend of the calculated data by Radke et al. and Douglas et al.

In order to probe the precision of our method, it seems rational to use our correction factors, *K*, to estimate absolute molecular weight data by multiplying *K* with the molecular weights from conventionally calibrated SEC. This approach is demonstrated in Fig. 10, in which both the uncorrected and corrected data from conventional SEC calibration are plotted together with the theoretically expected values. It can be clearly seen that the corrected molecular weights almost perfectly match the $\overline{M}_n^{\text{theo}}$ values, suggesting that our procedure is capable of yielding true molecular weights of star polymers. In order to finally prove that the perfect match between the corrected experimental values and the predicted molecular weights is not a coincidence, we measured absolute molecular weights of selected star polymer samples after SEC separation using a triple-detection system that comprised an RI, a viscometry, and a light-scattering detector. Fig. 10 shows convincingly that the absolute molecular weights perfectly blend into the data obtained using the introduced correction method.

The concise picture that is obtained for Z-RAFT star polymerization of styrene up to 6 arms and using phenylethyl as the leaving group allows the following conclusions to be drawn.

1. The number of arms of star polymer is constant above 30% of monomer conversion.
2. The number of arms is identical to the functionality of the star-shaped RAFT agent, i.e., all RAFT groups have initiated arm growth.
3. Even at very high monomer conversions (thus yielding large star molecules), there is no shielding effect observable that hampers the RAFT process. Otherwise, deviations from theoretical predictions would occur.

Having now a method at hand to correctly determine molecular weights of star polymers, we can evaluate the chain-transfer constant, C_{RAFT}, of the initial RAFT step. From a plot of the inverse number average degree of polymerization of one individual arm against the concentration of trithiocarbonate groups, C_{RAFT} can be evaluated via linear fitting according to the procedure introduced by Barner-Kowollik and co-workers [50,51]. Inspection of Fig. 1b shows that good linear behavior is observed in such a plot, from which a $C_{\text{RAFT}} = 164$ for phenylethyl-trithiocarbonate in styrene polymerization at 80 °C can be estimated. This relatively large value is indicative of a very effective chain transfer.

We also applied our method for obtaining apparent number of arms to Z-RAFT star polymerizations having benzyl as the leaving group. This study was inspired by the fact that all literature reports about Z-RAFT star polymerization of styrene used benzyl as the leaving group. When applying exactly the same experimental conditions and evaluation procedures as above, but using benzyl instead of phenylethyl as R-group, a completely different picture is obtained, as can be seen in Fig. 11. The apparent arm numbers are steadily increasing with monomer conversion and do reach the expected and confirmed values for the anticipated arm numbers – indicated by the horizontal dashed lines – only at very high *X* values, if at all. As the chemical nature of these stars and the solvent are unaltered, the strong deviations from the star polymers described above imply that the polymers from benzyl-type star-shaped RAFT agents have a distinctly different topology. The data suggest that the real arm numbers are well below the expected values and only slowly approach the expected numbers. Stenzel and co-workers made similar observations in Z-RAFT star polymerizations with benzyl-trithiocarbonates already in one of their

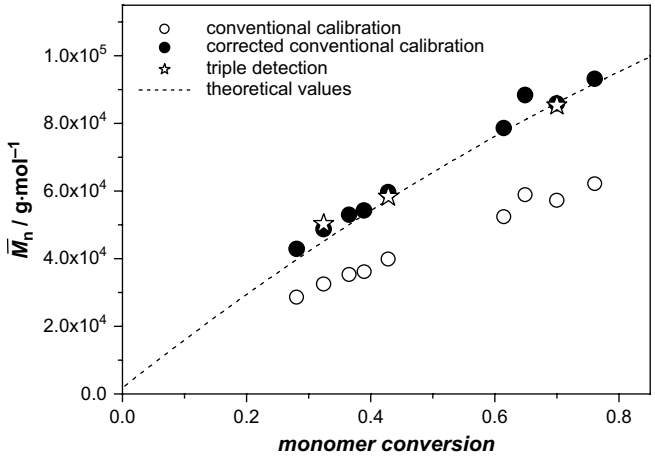

Fig. 10. Number average molecular weight, $\overline{M}_n$, of six-arm star polymer (data taken from Fig. 6) vs. monomer conversion, obtained via conventional SEC calibration (raw data and corrected by *K* given in Fig. 9) and via triple detection. The dashed line marks the theoretical molecular weight according to Eq. (1).

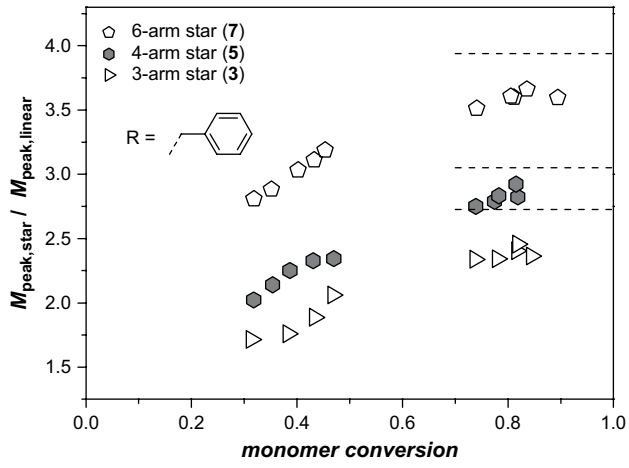

Fig. 11. Ratio of peak molecular weights of star polymers and peak molecular weights of linear arm polymers ($M_{\text{p,star}}/M_{\text{p,arm}}$; representing the apparent number of arms in conventionally calibrated SEC) vs. monomer conversion, from styrene bulk polymerizations at 80 °C using ACCN ($c_{\text{ACCN}} = 3$ mmol L^{-1}) as the initiator and mixtures of **1** and **3** (3-arm star polymerization), **1** and **5** (4-arm star polymerization), and **1** and **7** (6-arm star polymerization). The overall trithiocarbonate-group concentration was around 38 mmol L^{-1} for all samples with approximately half the number of RAFT groups belonging to multifunctional RAFT agents. Horizontal lines indicate the average values from Fig. 8.

early publications [20], in which they found evidence for an increasing number of arms with proceeding reaction. However, they did not quantify this effect, since they measured only apparent molecular weights of star polymers. Surprisingly, this worrying effect was not considered since then and benzyl-type star-shaped RAFT agents were uncritically used by many research groups. It may hence be that many observations, which were attributed to the mechanism of Z-RAFT star polymerization, simply stem from an inefficient pre-equilibrium, which apparently is highly relevant for the final topology.

It seems to be clear that the imperfect pre-equilibrium when using benzyl as the leaving group hampers the rapid initiation of arm growth, which apparently not only affects polydispersity, but more importantly, the topology of the final star polymer product. This dramatic effect is due to the multifunctionality of the star-shaped RAFT agent, which effectively needs to be initiated several times in a row before becoming a star. Unfortunately, our method for obtaining true molecular weights of star polymers is not able to detect apparent arm numbers at very low monomer conversions, as linear and star polymer species are not well separated in this regime. In order to fill this gap and to study the topologically evolution of star growth also in more effective systems, detailed theoretical and experimental studies of arm growth initiation at low monomer conversions are underway in our laboratory.

4. Conclusion

Z-RAFT star polymerization of styrene leading to star polymers having 3, 4, and 6 arms show very well controlled behavior up to very high monomer conversion. The application of high pressure up to 2600 bar could suppress the amount of dead polymer by more than a factor of 2.5, which is especially important for systems with low RAFT agent concentrations, where the fraction of terminated linear polymer may become substantial. No shielding effects were observed that would obstruct the RAFT process, not even at very high monomer conversions (yielding large star molecules). By using a mixture of linear and star-shaped RAFT agents, we were able to determine precise absolute molecular weights of star polymers using a conventionally calibrated SEC setup. When using trithiocarbonate-type RAFT agents with phenylethyl as the leaving group, a rapid chain transfer of the initial RAFT step was found and well-defined star polymers were formed, which perfectly match the theoretical predictions. However, when using benzyl as the leaving group in the star-shaped RAFT agents, a pronounced impact of monomer conversion on the number of arms was observed. It was found to be impossible to synthesize pure polystyrene star polymers with the expected number of arms, when using benzyl as the leaving group.

Acknowledgements

Financial support by the *Deutsche Forschungsgemeinschaft* for project VA226/3-1 and within the frame of the European Graduate School "Microstructural Control in Free-Radical Polymerization" is gratefully acknowledged. P.V. acknowledges receipt of a Heisenberg-Professorship (DFG). R.E. would like to thank the Dutch Polymer Institute for funding project no. 509 Cobra (comprehensive characterization of branched polymers) and Polymer Laboratories for making available a chip-based viscometer for the triple-detection measurements. Wim Kok (University of Amsterdam) is gratefully acknowledged for helpful discussions.

References

[1] Tezuka Y, Oike H. Prog Polym Sci 2002;27:1069–122.
[2] Lee JH, Goldberg JM, Fetters LJ, Archer LA. Macromolecules 2006;39:6677–85.
[3] McLeish TCB. Chem Eng Res Des 2000;78:12–32.
[4] Hadjichristidis N, Pispas S, Pitsikalis M, Iatrou H, Vlahos C. Asymmetric star polymers: synthesis and properties. In: Branched polymers I, vol. 142; 1999. p. 71–127.
[5] Li JS, Modak PR, Xiao HN. Colloids Surf A 2006;289:172–8.
[6] Qiu LY, Bae YH. Pharm Res 2006;23:1–30.
[7] Jones MC, Ranger M, Leroux JC. Bioconjug Chem 2003;14:774–81.
[8] Jie P, Venkatraman SS, Min F, Freddy BYC, Huat GL. J Controlled Release 2005;110:20–33.
[9] Fichter TM, Zhang L, Kiick KL, Reineke TM. Bioconjug Chem 2008;19:76–88.
[10] Likos CN. Soft Matter 2006;2:478–98.
[11] Vlassopoulos D, Fytas G, Pakula T, Roovers J. J Phys Condens Matter 2001;13:R855–76.
[12] Freire JJ. Adv Polym Sci 1999;143:35–112.
[13] Chiefari J, Chong YK, Ercole F, Krstina J, Jeffery J, Le TPT, et al. Macromolecules 1998;31:5559–62.
[14] Barner-Kowollik C, Davis TP, Heuts JPA, Stenzel MH, Vana P, Whittaker M. J Polym Sci Part A Polym Chem 2003;41:365–75.
[15] Moad G, Rizzardo E, Thang SH. Aust J Chem 2005;58:379–410.
[16] Perrier S, Takolpuckdee P. J Polym Sci Part A Polym Chem 2005;43:5347–93.
[17] Moad G, Rizzardo E, Thang SH. Aust J Chem 2006;59:669–92.
[18] Stenzel-Rosenbaum M, Davis TP, Chen V, Fane AG. J Polym Sci Part A Polym Chem 2001;39:2777–83.
[19] Mayadunne RTA, Jeffery J, Moad G, Rizzardo E. Macromolecules 2003;36:1505–13.
[20] Stenzel MH, Davis TP. J Polym Sci Part A Polym Chem 2002;40:4498–512.
[21] Darcos V, Dureault A, Taton D, Gnanou Y, Marchand P, Caminade AM, et al. Chem Commun (Cambridge, UK) 2004:2110–1.
[22] Boschmann D, Vana P. Polym Bull (Heidelberg, Ger) 2005;53:231–42.
[23] Bernard J, Favier A, Zhang L, Nilasaroya A, Davis TP, Barner-Kowollik C, et al. Macromolecules 2005;38:5475–84.
[24] Hao XJ, Malmstrom E, Davis TP, Stenzel MH, Barner-Kowollik C. Aust J Chem 2005;58:483–91.
[25] Boschmann D, Vana P. Macromolecules 2007;40:2683–93.
[26] Hong CY, You YZ, Liu J, Pan CY. J Polym Sci Part A Polym Chem 2005;43:6379–93.
[27] Chaffey-Millar H, Stenzel MH, Davis TP, Coote ML, Barner-Kowollik C. Macromolecules 2006;39:6406–19.
[28] Zhou GC, He JB, Harruna II. J Polym Sci Part A Polym Chem 2007;45:4225–39.
[29] Liu O, Chen Y. Macromol Chem Phys 2007;208:2455–62.
[30] Jesberger M, Barner L, Stenzel MH, Malmstrom E, Davis TP, Barner-Kowollik C. J Polym Sci Part A Polym Chem 2003;41:3847–61.
[31] Barner-Kowollik C, Davis TP, Stenzel MH. Aust J Chem 2006;59:719–27.
[32] Dureault A, Taton D, Destarac M, Leising F, Gnanou Y. Macromolecules 2004;37:5513–9.
[33] Frohlich MG, Vana P, Zifferer G. J Chem Phys 2007;127.
[34] Frohlich MG, Vana P, Zifferer G. Macromol Theory Simul 2007;16:610–8.
[35] Drache M, Boschmann D, Vana P, in preparation.
[36] Mänz M, Vana P, in preparation.
[37] Haney M, Jackson C, Yau W. In: Proceedings of the 1991 international GPC symposium; 1991. p. 49–63.
[38] Huang Y, Peng H, Lam JWY, Xu ZD, Leung FSM, Mays JW, et al. Polymer 2004;45:4811–7.
[39] Buback M, Frauendorf H, Vana P. J Polym Sci Part A Polym Chem 2004;42:4266–75.
[40] Bernard J, Hao XJ, Davis TP, Barner-Kowollik C, Stenzel MH. Biomacromolecules 2006;7:232–8.
[41] Johnston-Hall G, Monteiro MJ. Macromolecules 2008;41:727–36.
[42] Arita T, Buback M, Janssen O, Vana P. Macromol Rapid Commun 2004;25:1376–81.
[43] Barner-Kowollik C, Buback M, Charleux B, Coote ML, Drache M, Fukuda T, et al. J Polym Sci Part A Polym Chem 2006;44:5809–31.
[44] Mayadunne RTA, Rizzardo E, Chiefari J, Krstina J, Moad G, Postma A, et al. Macromolecules 2000;33:243–5.
[45] Chong YK, Krstina J, Le TPT, Moad G, Postma A, Rizzardo E, et al. Macromolecules 2003;36:2256–72.
[46] Barner-Kowollik C, Quinn JF, Nguyen TLU, Heuts JPA, Davis TP. Macromolecules 2001;34:7849–57.
[47] Quinn JF, Barner L, Davis TP, Thang SH, Rizzardo E. Macromol Rapid Commun 2002;23:717–21.
[48] Beuermann S, Buback M. Prog Polym Sci 2002;27:191–254.
[49] Initiators for high polymers. AKZO Nobel Chemicals; 2006.
[50] Theis A, Feldermann A, Charton N, Stenzel MH, Davis TP, Barner-Kowollik C. Macromolecules 2005;38:2595–605.
[51] Johnston-Hall G, Theis A, Monteiro MJ, Davis TP, Stenzel MH, Barner-Kowollik C. Macromol Chem Phys 2005;206:2047–53.
[52] Buback M, Frauendorf H, Günzler F, Huff F, Vana P, in preparation.
[53] Burchard W. Solution properties of branched macromolecules. In: Branched polymers I, vol. 143; 1999. p. 113–94.
[54] Douglas JF, Roovers J, Freed KF. Macromolecules 1990;23:4168–80.
[55] Radke W, Gerber J, Wittmann G. Polymer 2003;44:519–25.
[56] Radke W. Macromol Theory Simul 2001;10:668–75.
[57] Strazielle C, Herz J. Eur Polym J 1977;13:223–33.
[58] Strazielle C, Benoit H, Vogl O. Eur Polym J 1978;14:331–4.
[59] Stockmayer WH, Fixman M. Ann N Y Acad Sci 1953;57:334–52.
[60] Tsitsilianis C, Ktoridis A. Macromol Rapid Commun 1994;15:845–50.